Available online at www.sciencedirect.com

Manufacturing Letters

Manufacturing Letters 35 (2023) 523–528

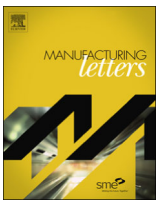

51st SME North American Manufacturing Research Conference (NAMRC 51, 2023)

Conformal Aerosol Jet Printing Using a 3-Axis Printer

Anushrut Jignasu[a], Jeremy D. Rurup[a], Ethan B. Secor[a], Adarsh Krishnamurthy[a,*]

[a]*Department of Mechanical Engineering, Iowa State University, Ames IA 50014, USA*

Abstract

Conformal patterning using contact printing methods has been problematic, owing to the complex topography of realistic surfaces and the sensitivity of print quality to the nozzle-substrate distance. Motion planning for such printing configurations is also a challenge, with conventional methods using tessellated representations to generate conformal toolpaths. However, these representations are often subject to truncation errors, thus diminishing the accuracy of the printed part. We propose and demonstrate a novel method to perform conformal aerosol jet printing on curved and topographically complex surfaces. We begin with a non-uniform rational B-spline (NURBS) definition of a surface, perform patch selection (i.e., area of interest) and extract its associated points and normals, and then generate GCode for conformal printing. We make use of a serpentine toolpath that resembles a strain-sensor pattern, thus suggesting the generalization of this method to conformal printing of circuits for applications in sensing, chemical analysis, thermal management, and pharmaceutical delivery with relative ease.

Keywords: Non-planar, Aerosol Jet Printing, NURBS, Conformal

1. Introduction

Digital printing technologies fuel a broad trend towards increasingly complex integration of electronic components. However, planar form factors remain dominant in practice due to simplicity in both the physical manufacturing process and the digital process planning tools [1]. Despite its challenge, compelling applications of conformal printing in wireless communication, structural health monitoring, bio-integrated electronics, and other areas continue to drive research interest in nonplanar printing technologies [2]. Contact printing methods, such as direct ink writing, pose challenges for conformal deposition due to their sensitivity to nozzle-surface distance and collision avoidance requirements. Among non-contact printing methods, aerosol jet printing (AJP) is a compelling technology due to its high standoff distance of 1-5 mm, high-resolution capability ($\approx 20\,\mu$m), and compatibility with electronically functional materials. For conformal printing, in particular, the standoff distance of AJP increases tolerance to nozzle-substrate misalignment, surface roughness, and machine compliance, which pose challenges to alternative patterning methods such as inkjet and electrohydrodynamic jet printing.

Alongside challenges in the physical deposition technologies, conformal printing requires sophisticated methods for process or trajectory planning. Defining a toolpath or print file presents a bottleneck in the process development and limits the utility of these methods that should, in principle, support rapid prototyping. Streamlined methods to program motion sequences that account for the 3D surface geometry of the substrate are thus important for the advancement of conformal printing technologies, bridging this gap between CAD geometry and machine code. This demands creative approaches to geometry representation and path planning that extend beyond legacy methods developed for subtractive machining methods to support the broader array of additive, non-contact printing methods such as AJP.

* Corresponding author.
E-mail address: adarsh@iastate.edu (Adarsh Krishnamurthy).

Nomenclature

AJP	Aerosol Jet Printing
NURBS	Non-Uniform Rational B-Splines
GCode	Geometric Code
FDM	Fused Depostion Modeling
SLA	Stereolithography

Boundary representations (B-reps) are the de-facto standard for representing CAD geometry. CAD software primarily utilizes parametric formulations of curved surfaces to efficiently represent the geometries. The caveat is that these representations require additional geometric processing to generate tessellations (triangulation) for downstream tasks. However, owing to truncation errors common during tessellation, there are inaccuracies associated with the tessellated representations. By contrast, Non-uniform Rational B-splines (NURBS) eliminate this problem. Given that they are piece-wise continuous functions, they offer a level of control and accuracy that is unmatched. NURBS have been previously used to represent CAD models and slicing operations [3, 4] for layered manufacturing.

Traditional toolpath generation for extrusion 3D printing mainly involves planar motion since the printing is performed layer by layer, i.e., additive manner. Most 3D printing toolpath generation algorithms first slice the 3D CAD model and extract the contours for each layer. The toolpaths are then generated for the contour and infill operation. However, the Z coordinate for each layer remains the same, and the print head is moved only along the XY plane within each layer. For conformal AJP, the Z coordinate of the print head has to be moved in conjunction with the movement along the XY plane to maintain the standoff distance. Moving to a 5-axis system for AJP complicates the toolpath generation process while also increasing costs. Using a NURBS definition of the freeform surface in this paper allows us to compute the movement along all three coordinates required to correctly move the nozzle using a 3-axis printer. We simultaneously calculate the movements along all 3-directions from the NURBS surface definition and feed it to the printer to generate the appropriate toolpath motion.

In this paper, we propose a novel method to perform conformal aerosol jet printing using only a 3-axis standard 3D printer and leverage it for printing circuit patterns on topographically complex surfaces. Most current 3D printing techniques operate on triangular meshes and deposit material in a planar fashion. Triangular meshes can be considered an approximate representation of the original geometry, owing to the discretization errors experienced during the conversion from a boundary representation (utilized by major CAD software) to a tessellated representation. Additionally, planar material deposition is a consequence of traditional slicing algorithms and usually leads to the commonly known staircase effect for curved geometries. However, conformal material deposition paves the way for minimizing the staircase effect. In addition, our proposed method does not utilize the traditional slicing algorithms to generate toolpaths but relies on a well-defined NURBS representation of a geometry.

Our novelty lies in utilizing a NURBS definition for a geometry to accomplish conformal 3D printing. Our main contributions include:

- A NURBS definition of the curved surface and selecting a local patch, (i.e., area of interest) and extraction of its associated points.
- GCode generation for conformal printing using a 3-axis printer.
- Application of this 3D printing method using a serpentine toolpath resembling an actual conformal sensor.

To our knowledge, the GCode generation for conformal printing using NURBS has not been done before, We demonstrate the viability of the approach by printing a serpentine pattern with conductive silver nanoparticle ink. Through this preliminary demonstration, we establish a foundation to extend this work to conformal printing of circuits for applications in sensing, chemical analysis, thermal management, and pharmaceutical delivery.

2. Background and Related Work

In aerosol jet printing (AJP), a functional ink is atomized to produce 1-5 micron droplets. A gas flow carries these droplets into a printhead, where a concentric sheath gas surrounds the aerosol stream and accelerates it through a deposition nozzle. The high velocity ($\approx 10 - 100$ m/s) aerosol jet remains focused for 1-5 mm beyond the nozzle exit, enabling the high standoff distance and approximately line-of-sight patterning crucial for conformal printing. By coupling the aerosol jet printhead with a digitally-controlled motion system, we can fabricate complex patterns in an additive manner.

Despite recognizing AJP as a highly promising candidate for conformal printing, even one-off demonstrations with idealized geometries (e.g., spheres and cylinders) require time-consuming fixture design, toolpath development, and alignment. Paulsen et al. [5] and Blumenthal et al. [6] were among the first to demonstrate the basic compatibility of AJP with a wide range of conformal electronics fabrication modalities, exploiting the high print offset, digital nature, and line-of-sight patterning of AJP. Gu et al. [7] followed with a more systematic and detailed approach to printing fillets for electrical interconnections between surfaces of different heights, a common challenge for microelectronics packaging. More recently, Vella et al. [8] and Gu et al. [9] provided thorough studies for printing functional electronics on well-defined 3D objects, including cylinders and cones, respectively, and Saeidi-Javash et al. [10] and Zeng et al. [11] demonstrated quasi-3D conformal AJP of 2D nanomaterials using a 3-axis printer. While these examples illustrate the promise of AJP for conformal electronics fabrication, they are constrained by traditional fabrication tools and inherently challenging to scale.

Non-uniform rational B-spline (NURBS) surfaces are the de facto standard for defining curved surfaces in CAD [12]. In our approach, we directly compute the toolpaths by defining a NURBS surface. Computing toolpaths on freeform surfaces is similar to the computation of fiber paths in composites, which has been investigated in previous studies [13, 14]. These studies are primarily interested in variable-stiffness composites, which are composite structures with curvilinear fiber paths that optimize the components' ability to withstand certain load requirements. Reference toolpaths can be found using a geodesic path, offset over the entire surface to determine parallel toolpaths [15]. Ravi Kumar et al. [16] investigated three different methods for computing geodesics on both (continuous, exact) and tessellated surfaces (discrete, approximate). They show that the most accurate method of computing geodesics is directly on the NURBS surface; however, most finite element analysis programs and computer-aided design models utilize tessellated file formats that do not provide a parameterized surface.

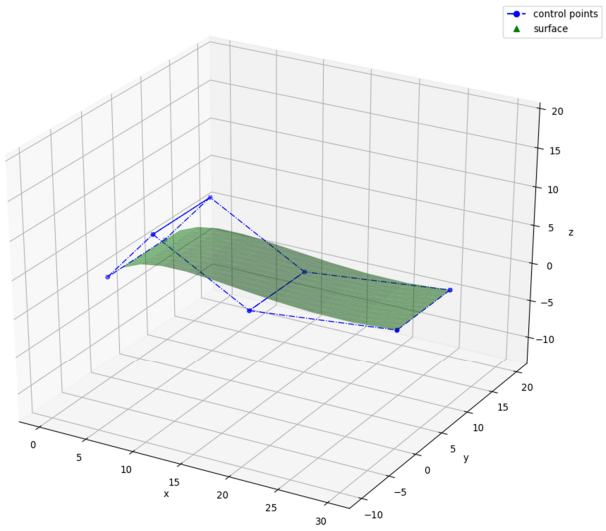

Fig. 1. NURBS surface generated using the NURBS-Python library.

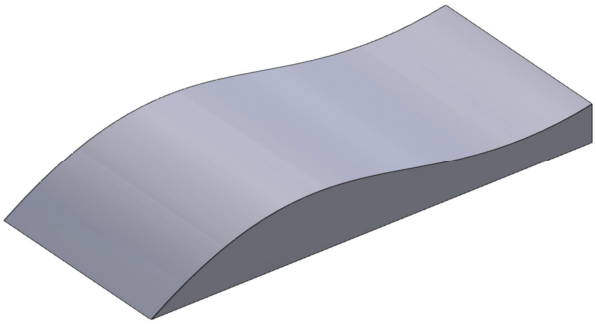

Fig. 2. Volume generated using the NURBS surface used to fabricate the substrate using SLA.

3. Method

In this paper, we propose a new method for conformal aerosol jet printing by leveraging the three degrees of freedom of an aerosol jet printer and the accuracy of NURBS representations for curved surfaces. We first describe the conformal AJP process for depositing inks onto a curved surface in Section 3.1, followed by the methodology for generating the curved toolpaths using NURBS in Section 3.2.

3.1. Aerosol Jet Printing

Printed electronics methods are unique from many other additive technologies in that functional, solid material is transported and deposited on the surface via a liquid ink. For aerosol jet printing, in particular, an aerosol is generated from a functional ink on our printer using a piezoelectric atomizer, transported to the printhead, and ejected from the nozzle with a gas flow, referred to as the carrier gas. A sheath gas is also introduced in the printhead, surrounding and focusing the aerosol-rich carrier gas flow. These are the primary controls to adjust the deposition rate and trace width on an aerosol jet printer.

3.2. NURBS Representation and GCode Generation

Formally, a point on the NURBS surface parametrized using (u, v) is defined as follows:

$$\mathbf{S}(u,v) = \frac{\sum_{i=0}^{n}\sum_{j=0}^{m} N_i^p(u) N_j^q(v) w_{ij} \mathbf{P}_{ij}}{\sum_{i=0}^{n}\sum_{j=0}^{m} N_i^p(u) N_j^q(v) w_{ij}}. \tag{1}$$

Here, the basis functions of NURBS, N_i^p, and N_j^q are polynomials recursively computed using Cox-de Boor recursion formula in Equation 2, where u is the parameter value and N_i^p is the i^{th} basis function of degree p.

$$N_i^p(u) = \frac{u - u_i}{u_{i+p} - u_i} N_i^{p-1}(u) + \frac{u_{i+p+1} - u}{u_{i+p+1} - u_{i+1}} N_{i+1}^{p-1}(u) \tag{2}$$

$$N_i^0(u) = \begin{cases} 1 & \text{if } u_i \le u \le u_{i+1} \\ 0 & \text{otherwise} \end{cases} \tag{3}$$

Here, u_i (also known as knots) refers to the elements of the knot vector $\mathbf{U}$ (similarly, $v_i \in \mathbf{V}$). The knot vector is a non-decreasing sequence of parametric coordinates, which divides the B-spline into non-uniform piecewise functions. The basis functions N_i^p spans over the parametric domain based on the knot vector and degree as shown in Equation 2 and Equation 3. Note that the formulation explained in Equation 1 uses the vector notation, where $\mathbf{P}_{ij}$ is embedded in $\Re^3$.

We define a B-spline surface with the same specifications as the deposition surface and then convert it to a NURBS surface. All operations are performed using the NURBS-Python library [17]. An example surface is shown in Fig. 1. Additionally, we export the outline of our curve in parametric u space into SolidWorks [18] and extrude along its width to generate a volume (shown in Fig. 2). We save this as an STL file and print using traditional SLA printing. This printed surface serves as our testbed for conformal printing.

Furthermore, for our experimental purposes, we select a patch on the NURBS surface (shown in Fig. 3(a)) and generate a serpentine pattern (shown in Fig. 3(b)). Given that we

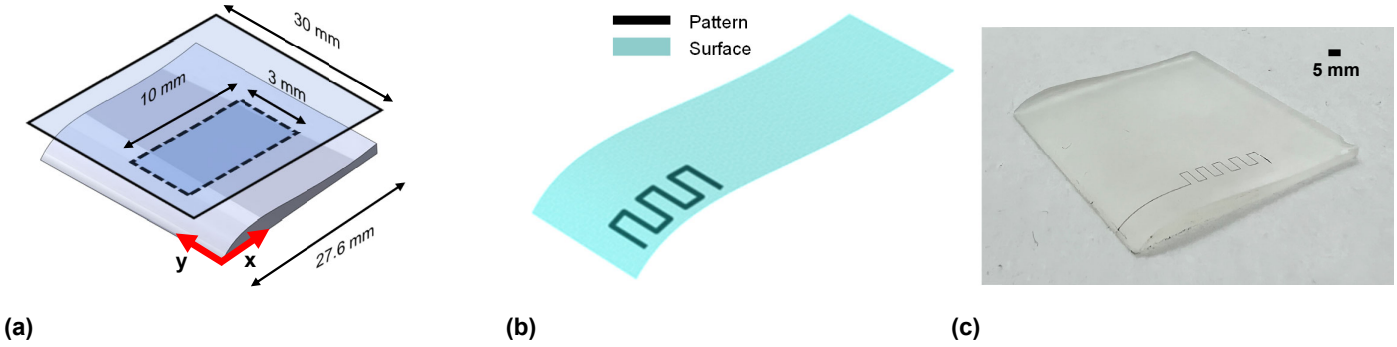

Fig. 3. Conformal printing of a serpentine pattern. (a) A region of interest projected onto the surface; (b) the serpentine pattern to be printed, and (c) the actual serpentine pattern printed using AJP onto a curved surface.

already possess the surface evaluation points for our NURBS surface, we define a knot span in the parametric *uv* space to get the points associated with the selected patch. Each point has X, Y, and Z coordinates associated with it, which we use for GCode generation. AJP is a non-contact additive manufacturing process, and all the surface points of the patch are offset by a standoff distance of 1-5 mm between the nozzle and the test part. AJP is relatively tolerant to variations in this surface offset distance, but substantial variations outside this range can negatively affect aerosol impaction on the surface and hence line resolution.

The toolpath generation algorithm remains the same for surfaces with higher degree curves in the parametric directions since we always have access to the evaluated surface points from the NURBS definition. Additionally, increasing the number of control points allows us to change the net geometry and should not affect the toolpath generation. Changing the knot vector offers an additional level of control over the local curvature of the geometry.

After generating the points lying on the patch, the next step is to generate toolpaths interpretable by the machine. Some additional commands are added specifically for AJP functionality. The most notable of these are the commands for feed rates and a shutter mechanism, which allows us to selectively turn the aerosol flow on and off. Our specific machine natively accepts the Galil DMC language, although GCode is a universal intermediary.

4. Results

We test our method on a simple serpentine pattern to demonstrate our conformal AJP printing capability from NURBS geometry. Our NURBS surface was generated using the NURBS-Python open-source library, and we used the surface evaluation points to identify points belonging to the region of interest by defining a knot span in the parametric *uv* space as shown in Fig. 3(a).

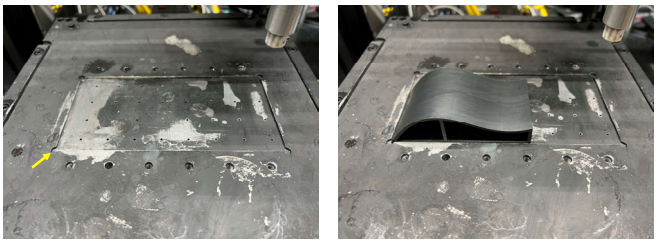

Fig. 4. Print bed with zero point (shown by yellow arrow, left) and the substrate aligned with the print bed.

The details of the NURBS surface are:

- Degree of curve in u direction: 3
- Degree of curve in v direction: 1
- Knot vector in u: [0.0, 0.0, 0.0, 0.0, 1.0, 1.0, 1.0, 1.0]
- Knot vector in v: [0.0, 0.0, 1.0, 1.0]
- Control points: [[0, 0, 0], [0, 10, 0], [5, 0, 7], [5, 10, 7], [15, 0, 0], [15, 10, 0], [30, 0, 2], [30, 10, 2]]
- Total surface evaluation points: 121

Printing was performed using a custom-built, 3-axis aerosol jet printer. The motion system comprises three linear motion stages, allowing for Cartesian motion in the XYZ directions, and is controlled via a Galil DMC-4040 motion controller. All printing was performed with a print speed of 5 mm/s, a nozzle diameter of 200 μm, a cartridge temperature of 20 °C, and a substrate temperature of 20 °C. We do not consider the print speed as part of the toolpath planning algorithm and leave it as an individual parameter with a fixed value. We set the aerosol and sheath gas flow rates to 12 and 60 sccm, respectively. The substrate was fabricated via SLA on a Formlabs Form2 printer using their general-purpose clear resin.

We do not require printer calibration and mount the substrate as shown in Fig. 4. We don't see an effect of the orientation of the substrate on the print quality as long as the slope of the substrate is not too high. The thickness of the substrate does not affect the toolpath generation since we zero the nozzle to the bottom left corner of the substrate before every print. The

Table 1. Quantitative comparison between a course STL model and a NURBS model.

Metric	Value (mm)
Model Height	2.500
Chamfer Distance	0.194

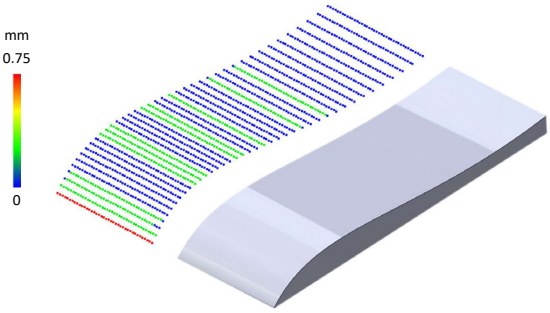

Fig. 5. The deviation from the NURBS model (left) and the STL model from a coarse tessellation (right).

NURBS definitions also use this point as the origin of the local coordinate system. We have only experimented with rigid substrates for aerosol deposition in this work, and the results are promising. The effect of non-rigid substrates remains to be explored.

A silver nanoparticle ink was prepared from a commercial ink obtained from UT Dots, Inc. (UTD-Ag25X), a dispersion of 25% w/v silver nanoparticles in xylenes. This was mixed with xylenes and terpineol in a ratio of 2:7:1 v/v UTD-Ag25X/xylenes/terpineol. Fig. 3(c) shows the resultant pattern printed on the conformal surface. The resulting example shows the viability of our approach to conformally print on complex curved surfaces. We maintain a constant standoff distance from the substrate; we are always within a tolerance of 1-5 mm (the most commonly used offset distance for AJP), thus keeping the width of deposition constant. Due to the oblique printing nature of our method, there may be a difference in the thickness of the aerosol deposited, and we leave the study of this as future work.

We illustrate the effect of the surface approximation error by using a coarse tessellation STL model for comparison against the NURBS surface. Note that this would be an exaggerated example since such a coarse tessellation will not be used in practice. However, the point of this example is to show that we can obtain higher accuracy with a more compact NURBS surface definition. We sample a point cloud of the coarse tessellation CAD model. We also generate a point cloud of the NURBS surface by densely sampling the surface. To illustrate the deviation of the STL model from the NURBS representation, we utilize CloudCompare [19]. Since we have a tessellated representation, we use the cloud-to-mesh distance measure to generate the color plot in Fig. 5. The error plot shows areas with higher curvature having a relatively larger deviation than areas with lower curvature. We make use of the one-sided Chamfer distance ($\mathcal{L}_{CD}$) metric to measure the deviation of the STL model from the NURBS surface. A general form of $\mathcal{L}_{CD}$ is shown in Equation 4. It is defined as the average of the distances between each point $\mathbf{P_i}$ in point set $\mathbf{P}$ and its nearest neighbor in point set $\mathbf{Q}$.

$$\mathcal{L}_{CD} = \sum_{\mathbf{P_i} \in \mathbf{P}} \min_{\mathbf{Q_j} \in \mathbf{Q}} \|\mathbf{P_i} - \mathbf{Q_j}\|_2 \tag{4}$$

It can be seen from Table 1 that the Chamfer distance is about 0.2 mm, which is almost 10% the model height. In addition, the maximum error could be as high as 0.75 mm at regions of higher curvature. This makes the STL representation not as suitable for path planning of AJP since this error is on the order of the nozzle offset distance, and the nozzle could collide with the substrate if the path is not carefully planned.

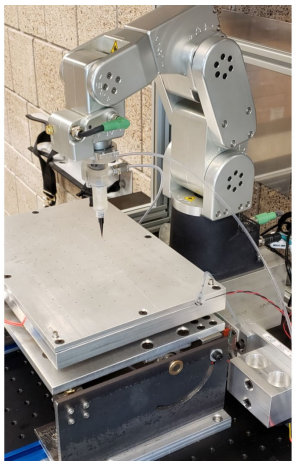

Fig. 6. Robotic arm with six degrees of freedom.

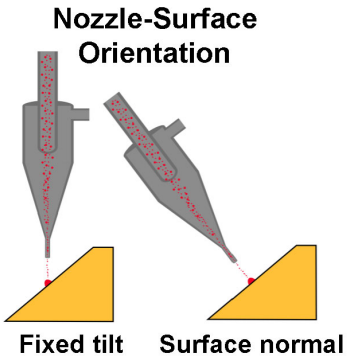

Fig. 7. Oblique deposition vs. surface-normal deposition for AJP.

5. Conclusions and Future Work

From the perspective of AJP physics, conformal printing on curved surfaces with a 3-axis motion system introduces an oblique jet orientation. Tolerance to this printing configuration is a key benefit of AJP and alters the constraints for suitable toolpath generation. During printing on a planar surface, with surface-normal nozzle orientation, the impinging jet has radial symmetry leading to symmetric deposition of aerosol droplets.

Breaking this symmetry, with nozzle orientation off-normal, alters not only the gas flow field but the droplet trajectories and potentially interfacial interactions between the gas flow and the coalesced liquid ink. Analyzing this effect on the quality and geometry of the final print would be one of the key future directions of this work.

Going forward, the ability to generate toolpaths over curved surfaces using a NURBS representation will support experiments to understand these constraints on the physical deposition process and how they reciprocally influence toolpath optimization. Furthermore, the generality of this methodology to more complex motion platforms, such as a 5-axis machine or 6-axis robot arm (shown in Fig. 6), by incorporating information of surface normals from the NURBS surface, would allow for direct comparison between surface-normal and oblique deposition on non-horizontal substrates (shown in Fig. 7).

A 5-axis machine or 6-axis robot arm can accomplish conformal printing on highly curved geometries, owing to their ability to align the nozzle to be normal to the surface, with their additional degrees of freedom. However, we do not have an explicit constraint for collision avoidance between the nozzle and substrate for highly curved geometries. We plan to incorporate collision detection algorithms to prevent unwanted collisions between the nozzle and the base geometry and maintain a uniform line resolution for the deposited aerosol. This general approach will thus enable streamlined and general technologies for conformal patterning of electronics with broad applications.

Acknowledgements

This work was supported by the National Science Foundation under grant number CMMI-2224303. We would like to thank Ankush Mishra at Iowa State University for his help with generating point cloud metrics.

References

[1] D. Hines, Y. Gu, A. Martin, P. Li, J. Fleischer, A. Clough-Paez, G. Stackhouse, A. Dasgupta, S. Das, Considerations of aerosol-jet printing for the fabrication of printed hybrid electronic circuits, Additive Manufacturing 47 (2021) 102325, ISSN 2214-8604.

[2] S. I. Rich, Z. Jiang, K. Fukuda, T. Someya, Well-rounded devices: the fabrication of electronics on curved surfaces – a review, Materials Horizons 8 (7) (2021) 1926–1958, ISSN 2051-6347, 2051-6355, doi:10.1039/D1MH00143D.

[3] P. Vuyyuru, C. Kirschman, G. Fadel, A. Bagchi, C. Jara-Almonte, A NURBS-based approach for rapid product realization, in: Proceedings of the 5th International Conference on Rapid Prototyping, The University of Dayton, 229–239, 1994.

[4] S. Sikder, A. Barari, H. Kishawy, Global adaptive slicing of NURBS based sculptured surface for minimum texture error in rapid prototyping, Rapid prototyping journal .

[5] J. A. Paulsen, M. Renn, K. Christenson, R. Plourde, Printing conformal electronics on 3D structures with aerosol jet technology, in: 2012 Future of Instrumentation International Workshop (FIIW) Proceedings, 1–4, doi:10.1109/FIIW.2012.6378343, 2012.

[6] T. Blumenthal, V. Fratello, G. Nino, K. Ritala, Conformal printing of sensors on 3D and flexible surfaces using aerosol jet deposition, in: Nanosensors, Biosensors, and Info-Tech Sensors and Systems, vol. 8691, International Society for Optics and Photonics, 86910P, doi:10.1117/12.2009278, 2013.

[7] Y. Gu, D. R. Hines, V. Yun, M. Antoniak, S. Das, Aerosol-jet printed fillets for well-formed electrical connections between different leveled surfaces, Advanced Materials Technologies 2 (11) (2017) 1700178, ISSN 2365-709X.

[8] S. Vella, C. S. Smithson, K. Halfyard, E. Shen, M. Chrétien, Integrated capacitive sensor devices aerosol jet printed on 3D objects, Flexible and Printed Electronics 4 (4) (2019) 045005, ISSN 2058-8585, doi:10.1088/2058-8585/ab59c0.

[9] Y. Gu, D. Park, D. Bowen, S. Das, D. R. Hines, Direct-write printed, solid-core solenoid inductors with commercially relevant inductances, Advanced Materials Technologies 4 (1) (2019) 1800312, ISSN 2365-709X.

[10] M. Saeidi-Javash, W. Kuang, C. Dun, Y. Zhang, 3D conformal printing and photonic sintering of high-performance flexible thermoelectric films using 2D nanoplates, Advanced Functional Materials 29 (35) (2019) 1901930, ISSN 1616-3028.

[11] M. Zeng, W. Kuang, I. Khan, D. Huang, Y. Du, M. Saeidi-Javash, L. Zhang, Z. Cheng, A. J. Hoffman, Y. Zhang, Colloidal nanosurfactants for 3D conformal printing of 2D Van der Waals materials, Advanced Materials 32 (39) (2020) 2003081, ISSN 1521-4095, doi:10.1002/adma.202003081.

[12] A. A. G. Requicha, J. R. Rossignac, Solid Modeling and Beyond, IEEE Computer Graphics Applications 12 (5) (1992) 31–44.

[13] S. Nagendra, S. Kodiyalam, J. Davis, V. Parthasarathy, Optimization of tow fiber paths for composite design, in: 36th Structures, Structural Dynamics and Materials Conference, American Institute of Aeronautics and Astronautics, 1031–1041, doi:10.2514/6.1995-1275, 1995.

[14] S. Setoodeh, A. Blom, M. Abdalla, Z. Gürdal, Generating curvilinear fiber paths from lamination parameters distribution, in: Structures, Structural Dynamics, and Materials Conference, American Institute of Aeronautics and Astronautics, ISBN 978-1-62410-040-6, 1875, doi:10.2514/6.2006-1875, 2006.

[15] N. Scheirer, S. Holland, A. Krishnamurthy, Fiber layup generation on curved composite structures, Computer-Aided Design 136 (2021) 103031.

[16] G. Ravi Kumar, P. Srinivasan, V. Devaraja Holla, K. Shastry, B. Prakash, Geodesic curve computations on surfaces, Computer Aided Geometric Design 20 (2) (2003) 119–133, ISSN 0167-8396.

[17] O. R. Bingol, A. Krishnamurthy, NURBS-Python: An open-source object-oriented NURBS modeling framework in Python, SoftwareX 9 (2019) 85–94, doi:https://doi.org/10.1016/j.softx.2018.12.005.

[18] SolidWorks Corp., SolidWorks, URL `www.solidworks.com`, 2021.

[19] CloudCompare, CloudCompare (version 2.11.3), URL `http://www.cloudcompare.org/`, 2022.